

Photoassisted Generation of a Dinuclear Iron(III) Peroxo Species and Oxygen-Atom Transfer**

Frédéric Avenier, Christian Herrero, Winfried Leibl, Alain Desbois, Régis Guillot, Jean-Pierre Mahy,* and Ally Aukauloo*

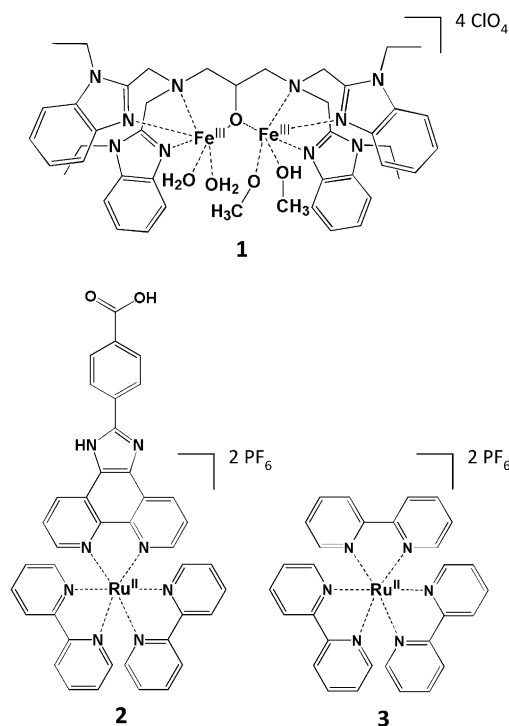
Dedicated to Harry B. Gray

Nature has developed a large variety of metalloenzymes capable of catalyzing selective oxidation reactions through the reductive activation of dioxygen at mono- or dinuclear iron active sites.^[1–4] Among these metalloenzymes, cytochromes P₄₅₀ (cytP₄₅₀), with a mononuclear iron active site, are the most widely known and studied, whereas soluble methane monooxygenase (MMO), which contains a dinuclear iron center, is under intensive investigation.^[5] Both systems oxidize a variety of organic substrates by the use of dioxygen and electrons provided by NAD(P)H to give the desired products and water. Much progress has been made in understanding the structure/function relationship of these metalloenzymes on the basis of synthetic systems,^[6–8] and key intermediates, such as high-valent iron–oxo^[9,10] and iron–peroxo species^[5] have been identified and characterized. However, in most of these synthetic models, the high-valent iron–oxo or iron–peroxo species were generated by the addition of chemical oxidants, such as PhIO, H₂O₂, or O₂, in the presence of electron and proton donors. Gray and co-workers were the first to photogenerate different intermediates of cytP₄₅₀ through a photosensitizer–cytP₄₅₀ assembly in the presence or the absence of electron scavengers.^[11–14] Meanwhile, Fukuzumi, Nam, and co-workers reported the photocatalytic generation of high-valent iron–oxo species by the use of water as an oxygen-atom source in the presence of sacrificial electron acceptors.^[15,16] An appealing alternative for the formation of such active species would be a photo-reductive process with O₂.^[17]

Herein, we report the photocatalytic activation of O₂ at a diiron(II) complex upon irradiation of a system composed of the corresponding diiron(III) complex, a ruthenium(II)–

polybipyridine-type complex, which acts as a photosensitizer, and triethylamine (TEA), which functions as a sacrificial electron donor. Exposure of the photogenerated diiron(II) complex to O₂ leads to the formation of the diiron(III)–peroxo intermediate responsible for oxygen-atom transfer to a substrate.

The dinucleating ligand *N,N,N',N'*-tetrakis(*N*-ethyl-2-benzimidazolylmethyl)-2-hydroxy-1,3-diaminopropane (*N*-EtHPTB)^[18] used to form complex **1** (Scheme 1) has commonly been used to develop synthetic models for MMO, and



Scheme 1. Structures of the diiron complex **1** and ruthenium complexes **2** and **3** used in this study.

has been particularly useful for studying the formation of diiron(III)–μ-1,2-peroxo species by exposure of the corresponding carboxylate-bridged diiron(II) complexes to O₂.^[19–23]

Our strategy to build a molecular assembly with an *N*-EtHPTB–diiron complex involved the preparation of the corresponding diiron(III) complex **1** without a bridging carboxylate group and thus with free coordination sites for

[*] Dr. F. Avenier, Dr. C. Herrero, Dr. R. Guillot, Prof. J.-P. Mahy, Prof. A. Aukauloo
Institut de Chimie Moléculaire et des Matériaux d'Orsay
(UMR CNRS 8182), Université Paris Sud
Orsay, 91405 CEDEX (France)
E-mail: jean-pierre.mahy@u-psud.fr
ally.aukauloo@u-psud.fr

Dr. C. Herrero, Dr. W. Leibl, Dr. A. Desbois, Prof. A. Aukauloo
CEA, iBiTecS, UMR 8221
Service de Bioénergétique, Biologie Structurale et Mécanismes
91191 Gif-sur-Yvette (France)

[**] We thank "l'Agence Nationale de la Recherche" (ANR TECHBIO-PHYP, ANR CATHYMETOXY) and the Labex project CHARMMAT for financial support.

Supporting information for this article is available on the WWW under <http://dx.doi.org/10.1002/anie.201210020>.

the carboxylate group of ruthenium complex **2**^[24] (Scheme 1). Complex **1** was prepared by mixing the *N*-EtHPTB ligand with iron(III) perchlorate (2 equiv); slow evaporation of the resulting solution in methanol yielded crystals of sufficient quality for X-ray crystal-structure analysis. Interestingly, the structure of **1** (Figure 1) features two different coordination

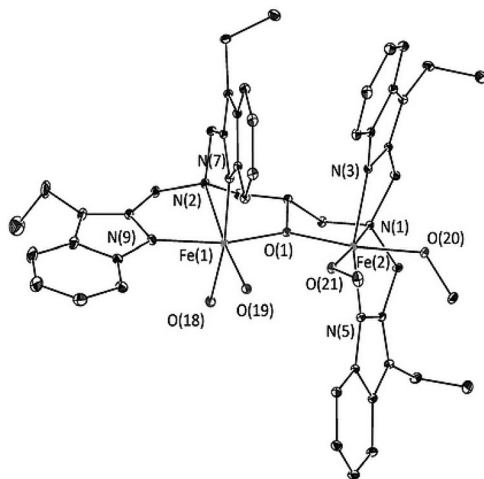


Figure 1. X-ray crystal structure of complex **1**: $[\text{Fe}^{\text{III}}_2(\text{N-EtHPTB})(\text{H}_2\text{O})_2(\text{CH}_3\text{O})(\text{CH}_3\text{OH})](\text{ClO}_4)_4$.

spheres for the iron(III) centers. Fe(1) holds two water molecules and two benzimidazole groups positioned in a *cis* configuration, whereas Fe(2) bears two methanol molecules and two benzimidazole fragments in a *trans* configuration. The different distances of 1.87 and 2.07 Å between Fe(2) and the two methanol molecules indicate that one of the methanol molecules is deprotonated.

Prior to our studies of photoinduced electron transfer, we examined the reactivity of **1** with hydrogen peroxide. Upon the addition of H_2O_2 (10 equiv), the initial red solution of **1** in acetonitrile turned dark blue-green with a maximum absorption at 620 nm ($\epsilon = 2900 \text{ M}^{-1} \text{ cm}^{-1}$). This species was stable for minutes at room temperature. When the same experiment was performed at -40°C , a considerable gain in stability was observed for the same species (several hours), and only 1.5 equivalents of H_2O_2 were sufficient for complete transformation. No isosbestic points were observed when the reaction was monitored on the basis of time-resolved UV/Vis spectra upon the direct addition of H_2O_2 at low temperature. The absence of isosbestic points suggests the existence of an additional chemical step. Conversely, when the initial solution of **1** was first treated with HClO_4 (1 equiv), we observed a sharpening of the absorption bands of the starting material, and the subsequent addition of H_2O_2 led to the formation of two isosbestic points, which indicated that no secondary reaction took place within the considered time range (Figure 2). The effect of acid was further investigated by the titration of **1** with HClO_4 (see Figure S1 in the Supporting Information). A one-step transformation with only 0.5 equivalents of the acid was observed, which suggests that about 50% of the methanol ligand is in the deprotonated form, as inferred from the X-ray crystal structure. Together, these

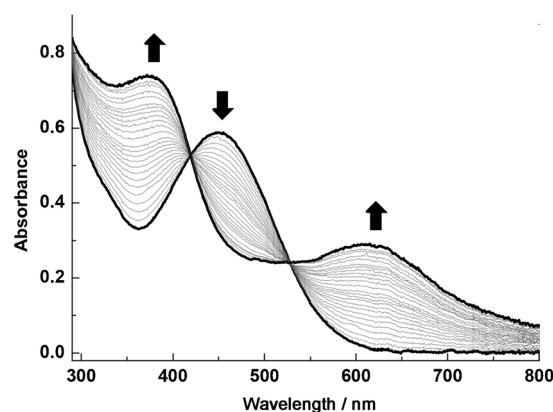


Figure 2. UV/Vis spectral changes of a solution of complex **1** in acetonitrile upon the addition of H_2O_2 at -40°C over a period of 1 h ($[\text{I}] = 0.1 \text{ mM}$, $[\text{H}_2\text{O}_2] = 1 \text{ mM}$, $[\text{HClO}_4] = 0.1 \text{ mM}$).

findings support the hypothesis that **1** is first partly protonated at one methanolate site and then reacts with the peroxide to form the diiron(III)- μ -1,2-peroxo intermediate; this reactivity is reminiscent of that of similar iron complexes.^[25] The diiron(III)- μ -1,2-peroxo intermediate was characterized by resonance Raman spectroscopy. Raman bands were observed at 467/477 cm^{-1} in the region corresponding to symmetric Fe–O stretching and at 881/896/910 cm^{-1} (Fermi-coupled stretching according to Do et al.)^[23] in the O–O stretching region. (see Figure S2 in the Supporting Information).

Crystallization attempts with an equimolar solution of **1** and **2** (Scheme 1) did not yield any crystal of the expected supramolecular adduct. However, spectral changes in the vibrational frequencies of the pendent carboxylate group of **2** clearly demonstrate the binding of **2** to the diiron core (see Figure S3 in the Supporting Information). With the goal of the photoreduction of the diiron(III) core of **1** to the diiron(II) derivative and concomitant activation of O_2 , we subjected an equimolar solution of **1** and **2** in the presence of excess TEA as an electron donor to a cycle of deoxygenation, irradiation at 460 nm, and exposure to O_2 (bubbled through the solution). Figure 3 shows the UV/Vis spectra recorded after each cycle and demonstrates that exposure to dioxygen, after irradiation with light at 460 nm, generates an absorption shoulder at about 600 nm, which suggests the formation of a new species that does not appear in the absence of the iron complex (see Figure S4 in the Supporting Information). The differential of the electronic absorption spectra before and after exposure to O_2 clearly shows a band at about 590 nm (Figure 3, inset). This band is comparable to the absorption spectrum of the peroxo intermediate chemically generated as described above, but is slightly shifted to a higher energy. However, its maximum matches that found for other diiron(III)- μ -peroxo species obtained from carboxylato bridging complexes of the same ligand.^[20,23] These findings support the generation of the diiron(III)-peroxo intermediate through the cycle of excitation with light and exposure to O_2 .

On the basis of previous studies on the reactivity of diiron(III)- μ -peroxo species,^[21] we treated the photogenerated diiron(III)- μ -peroxo species with a stoichiometric amount of Ph_3P . Mass spectrometric analyses showed the

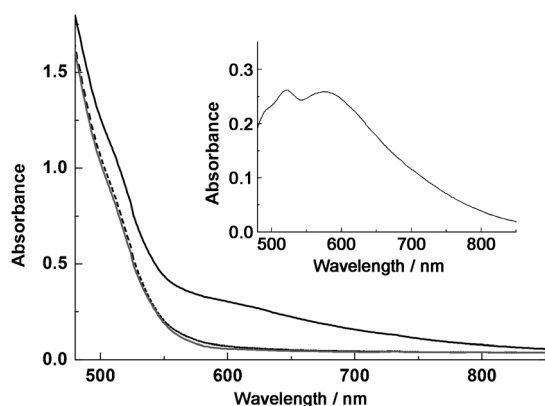
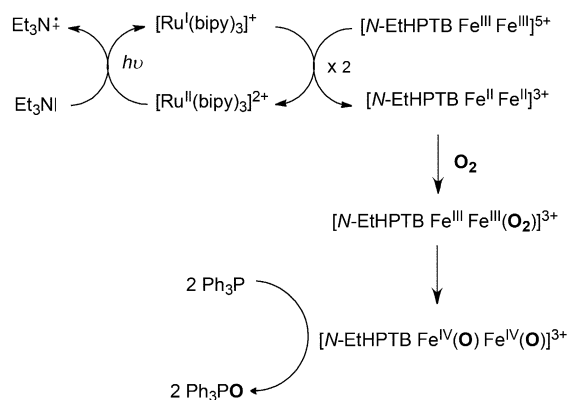


Figure 3. UV/Vis spectra of complexes **1** and **2** with Et₃N in deoxygenated acetonitrile before irradiation (dashed black line), after irradiation at 460 nm for 20 min (solid gray line), and after irradiation followed by exposure to O₂ (solid black line); [1] = 0.1 mM, [2] = 0.1 mM, [Et₃N] = 10 mM, −10 °C). Inset: Differential spectrum obtained by subtracting the spectrum obtained before exposure to O₂ (solid gray line) from the spectrum obtained after exposure to O₂ (solid black line).

formation of Ph₃PO in relatively small amounts, and further experiments with three successive cycles of irradiation led to about 80 % conversion of the Ph₃P into Ph₃PO (see Figure S5 in the Supporting Information). To confirm that the system was able to perform multiturnover catalysis, we then treated it with 10 equivalents of Ph₃P, and the amount of Ph₃PO formed was measured by HPLC after each photocatalytic cycle.

The photocatalytic cycle involving a combination of complexes **1** and **2** (Scheme 2) generates Ph₃PO linearly as a function of the number of cycles, and a Ph₃PO concentration of about 1.8 mM is reached after 5 cycles (Figure 4). Consid-



Scheme 2. Suggested mechanism for photoinduced dioxygen activation at a dinuclear iron(III) complex and subsequent oxygen-atom transfer.

ering that one diiron complex can potentially generate two iron(IV)–oxo entities (Scheme 2), this amount of Ph₃PO corresponds to a yield of about 36 %. Surprisingly, the same experiment with complexes **1** and **3**^[26] (Scheme 1) led to an improvement in the observed yield for the oxidation of Ph₃P to about 60 % after 5 cycles. This difference in reactivity between **2** and **3** can be explained by the presence of the

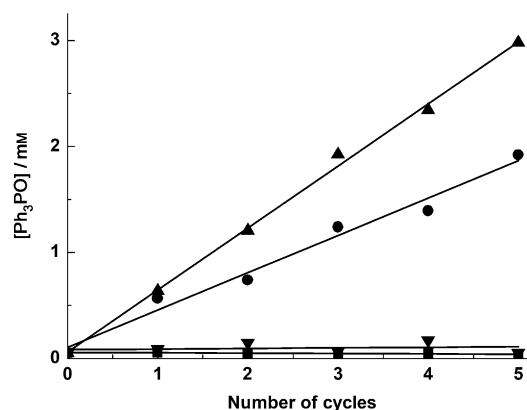


Figure 4. Production of Ph₃PO from Ph₃P in successive photocatalytic cycles involving 1) deoxygenation of the solution, 2) irradiation under a controlled atmosphere at 460 nm (20 min), and 3) bubbling of O₂ through the solution (20 min): ● catalysis with complexes **1** and **2**; ▲ catalysis with complexes **1** and **3**; ■ control without the ruthenium complex (no irradiation); ▼ control without **1**. Reaction conditions: [1] = 0.5 mM, [2] or [3] = 0.5 mM, [Et₃N] = 50 mM, [Ph₃P] = 5 mM, MeCN (solvent), room temperature.

imidazole group between the chromophore and the carboxylate binding group in complex **2**. Laser flash photolysis studies on **2** showed that the imidazole group is deprotonated in the presence of TEA, which leads to deactivation of the Ru-based triplet state.^[27] As a result, the lifetime of the excited state of **2** is shorter than that of **3** (270 versus 670 ns; see Figure S6 in the Supporting Information). Consequently, considerably less photoreduced Ru^I is formed by reaction with the sacrificial electron donor (see Figure S7 in the Supporting Information), and the yield of the reaction is lower. Further studies on the synthesis of chromophores bearing carboxylate groups to enhance vectorial electron transfer are under way.

In summary, we have described the photoreduction of a diiron(III) mimic of MMO in the presence of a sacrificial electron donor. The photoreduced diiron(II) complex reacted with O₂ to generate a diiron(III) peroxo species that was able to transfer an oxygen atom to a substrate.

Received: December 14, 2012

Revised: January 23, 2012

Published online: February 20, 2013

Keywords: dioxygen activation · iron complexes · peroxo intermediates · photoreduction · ruthenium complexes

- [1] B. Meunier, S. P. de Visser, S. Shaik, *Chem. Rev.* **2004**, *104*, 3947–3980.
- [2] L. Que, R. Y. N. Ho, *Chem. Rev.* **1996**, *96*, 2607–2624.
- [3] B. J. Wallar, J. D. Lipscomb, *Chem. Rev.* **1996**, *96*, 2625–2658.
- [4] M. Merckx, D. A. Kopp, M. H. Sazinsky, J. L. Blazyk, J. Müller, S. J. Lippard, *Angew. Chem.* **2001**, *113*, 2860–2888; *Angew. Chem. Int. Ed.* **2001**, *40*, 2782–2807.
- [5] C. E. Tinberg, S. J. Lippard, *Acc. Chem. Res.* **2011**, *44*, 280–288.
- [6] E. Y. Tshuva, D. Lee, W. Bu, S. J. Lippard, *J. Am. Chem. Soc.* **2002**, *124*, 2416–2417.

- [7] I. Siewert, C. Limberg, *Chem. Eur. J.* **2009**, *15*, 10316–10328.
- [8] S. Friedle, E. Reisner, S. J. Lippard, *Chem. Soc. Rev.* **2010**, *39*, 2768–2779.
- [9] C. Krebs, D. Galonić Fujimori, C. T. Walsh, J. M. Bollinger, *Acc. Chem. Res.* **2007**, *40*, 484–492.
- [10] L. Que, Jr. *Acc. Chem. Res.* **2007**, *40*, 493–500.
- [11] A. R. Dunn, I. J. Dmochowski, J. R. Winkler, H. B. Gray, *J. Am. Chem. Soc.* **2003**, *125*, 12450–12456.
- [12] J. J. Wilker, I. J. Dmochowski, J. H. Dawson, J. R. Winkler, H. B. Gray, *Angew. Chem.* **1999**, *111*, 93–96; *Angew. Chem. Int. Ed.* **1999**, *38*, 89–92.
- [13] D. W. Low, J. R. Winkler, H. B. Gray, *J. Am. Chem. Soc.* **1996**, *118*, 117–120.
- [14] M. E. Ener, Y.-T. Lee, J. R. Winkler, H. B. Gray, L. Cheruzel, *Proc. Natl. Acad. Sci. USA* **2010**, *107*, 18783–18786.
- [15] S. Fukuzumi, T. Kishi, H. Kotani, Y.-M. Lee, W. Nam, *Nat. Chem.* **2011**, *3*, 38–41.
- [16] H. Kotani, T. Suenobu, Y.-M. Lee, W. Nam, S. Fukuzumi, *J. Am. Chem. Soc.* **2011**, *133*, 3249–3251.
- [17] N.-H. Tran, N. Huynh, T. Bui, Y. Nguyen, P. Huynh, M. E. Cooper, L. E. Cheruzel, *Chem. Commun.* **2011**, *47*, 11936–11938.
- [18] V. McKee, M. Zvagulis, J. V. Dagdigan, M. G. Patch, C. A. Reed, *J. Am. Chem. Soc.* **1984**, *106*, 4765–4772.
- [19] S. Menage, B. A. Brennan, C. Juarez-Garcia, E. Munck, L. Que, Jr., *J. Am. Chem. Soc.* **1990**, *112*, 6423–6425.
- [20] Y. Dong, S. Menage, B. A. Brennan, T. E. Elgren, H. G. Jang, L. L. Pearce, L. Que, Jr., *J. Am. Chem. Soc.* **1993**, *115*, 1851–1859.
- [21] Y. Dong, S. Yan, V. G. Young, Jr., L. Que, Jr., *Angew. Chem.* **1996**, *108*, 673–676; *Angew. Chem. Int. Ed. Engl.* **1996**, *35*, 618–620.
- [22] A. L. Feig, M. Becker, S. Schindler, R. van Eldik, S. J. Lippard, *Inorg. Chem.* **1996**, *35*, 2590–2601.
- [23] L. H. Do, T. Hayashi, P. Moënné-Loccoz, S. J. Lippard, *J. Am. Chem. Soc.* **2010**, *132*, 1273–1275.
- [24] A. J. Simaan, Y. Mekmouche, C. Herrero, P. Moreno, A. Aukauloo, J. A. Delaire, M. Réglie, T. Tron, *Chem. Eur. J.* **2011**, *17*, 11743–11746.
- [25] L. Westerheide, F. K. Müller, R. Than, B. Krebs, J. Dietrich, S. Schindler, *Inorg. Chem.* **2001**, *40*, 1951–1961.
- [26] V. Balzani, A. Juris, *Coord. Chem. Rev.* **2001**, *211*, 97–115.
- [27] A. Quaranta, F. Lachaud, C. Herrero, R. Guillot, M.-F. Charlot, W. Leibl, A. Aukauloo, *Chem. Eur. J.* **2007**, *13*, 8201–8211.